

Electric Field in a Plasma Channel in a High-Pressure Nanosecond Discharge in Hydrogen: A Coherent Anti-Stokes Raman Scattering Study

S. Yatom,¹ S. Tskhai,² and Ya. E. Krasik¹

¹*Department of Physics, Technion, Haifa 32000, Israel*

²*Lebedev Physics Institute, Russian Academy of Sciences, 117924 Moscow, Russia*

(Received 11 September 2013; published 18 December 2013)

Experimental results of a study of the electric field in a plasma channel produced during nanosecond discharge at a H_2 gas pressure of $(2-3) \times 10^5$ Pa by the coherent anti-Stokes scattering method are reported. The discharge was ignited by applying a voltage pulse with an amplitude of ~ 100 kV and a duration of ~ 5 ns to a blade cathode placed at a distance of 10 and 20 mm from the anode. It was shown that this type of gas discharge is characterized by the presence of an electric field in the plasma channel with root-mean-square intensities of up to 30 kV/cm. Using polarization measurements, it was found that the direction of the electric field is along the cathode-anode axis.

DOI: 10.1103/PhysRevLett.111.255001

PACS numbers: 52.80.-s, 42.65.Dr, 52.25.Jm, 52.70.-m

Nanosecond (ns) time scale electrical discharges in different gases at pressure $P \geq 10^5$ Pa have been widely investigated [1–8] due to the interesting physical phenomena involved. Such discharges are ignited by the application of high-voltage (HV) pulses with an amplitude in the range 10^4 – 10^5 V and a rise time of 10^{-10} – 10^{-9} s. It is supposed that runaway electrons (RAE) generated at the beginning of the discharge are responsible for preionization of the gas [9], allowing plasma discharge to be developed in a nanosecond time scale. The origin of RAE is still the subject of additional research and one of the key questions is the electric field's temporal and spatial distribution in the cathode-anode gap. It is commonly accepted that the source of RAE is the electron emission from cathode whiskers, where significant enhancement of the electric field is realized [4,6,10,11]. However, one cannot also exclude that the emission of RAE occurs from the front of the propagating plasma streamer having a micron scale size head or from the boundary of the plasma channel when it approaches the anode to a distance where the condition for the generation of RAE is fulfilled [4,12,13]. In the latter case, the conductivity of the plasma channel should be sufficiently large to allow the plasma to acquire the potential of the cathode. It was found that when plasma bridges the cathode-anode gap, the HV stage of discharge is not terminated [5,6], again raising the question of how conductive this plasma is. The conductivity of the plasma channel is also very important for estimating the energy dissipation and, respectively, the efficiency of different devices (pulsed power generators, microwave compressors, etc.) whose operation requires application of the plasma formed during a nanosecond time scale in pressurized gases.

Recent time- and space-resolved spectroscopic studies of the nanosecond time scale duration discharge in He gas at $P = 10^5$ Pa yielded values of the plasma electron density in the range of 10^{15} – 10^{16} cm⁻³ and very complex dynamics

of channel formation [14,15]. Detailed fitting of several spectral He lines has shown strong evidence of the presence of significant low-frequency (≤ 10 GHz) electric fields with a rms intensity of ~ 10 kV/cm inside the plasma channels [15].

Conventional approaches to the nonperturbing measurement of the electric field in plasmas, such as Stark broadening of spectral lines and fluorescence of Rydberg states [16–18], become rather complicated analytically at pressures at $P \geq 10^5$ Pa, since collisions with neutrals begin to be dominant for low-ionized plasma. Coherent anti-Stokes Raman scattering (CARS) has proved to be an efficient method for measuring the local electric field in plasmas and gases with a large concentration of hydrogen or nitrogen. The possibility of measuring a static electric field using the absorption of infrared (IR) photons in the induced spectrum of the rotation energy levels of diatomic molecules was theoretically predicted by Condon in 1932 [19] as a limiting case of the Raman effect. This prediction was confirmed in experiments by Crawford *et al.* in 1949 [20]. In 1991 the experimental setup for the measurement of an electric field by induced IR emission was proposed [21], and it was implemented several years later [22,23]. Recently, CARS was used to measure electric fields in dielectric barrier discharges with temporal resolution down to several nanoseconds [24]. CARS is based on the generation of coherent infrared radiation as a result of the biharmonic laser pumping of an initially symmetrical diatomic molecule in an external electric field. This electric field induces the dipole moment of the molecules and allows IR vibrational transitions in the dipole approximation. In the case of the H_2 molecule [see Fig. 1(a)], the infrared radiation is emitted at the frequency of the Raman-active vibrational-rotational transition $Q(1)$ ($\nu=0, J=1 \rightarrow \nu=1, J=1$) in the ground electronic state $X^1\Sigma_g^+$ ($\lambda = 2.4$ μm). The application of two biharmonic laser waves [ω_p and ω_s , see Fig. 1(a)] leads to coherent vibration ($\omega_p - \omega_s$) of

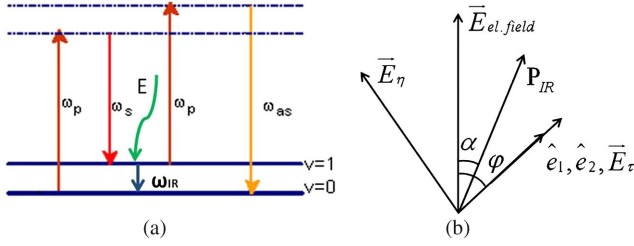


FIG. 1 (color online). (a) Optical transitions in degenerate CARS and generation of infrared signal due to electric field. (b) The idea behind the CARS polarization measurements.

the molecules with the induced $\nu = 0 \rightarrow \nu = 1$ transition, which causes inelastic scattering of one of the waves [for instance, ω_p in Fig. 1(a)]. This scattered wave ω_3 may have a different frequency (nondegenerate CARS, i.e., $\omega_p - \omega_s + \omega_3 = \omega_{as}$) and, in particular, this frequency may be zero, which corresponds to the case of a static electric field [25].

Theoretical analysis [23] showed that the value of the external electric field can be calculated as

$$E = C \sqrt{\frac{I_{ir}}{I_{CARS}}} I_p, \quad (1)$$

where I_{ir} is the intensity of IR signal induced by the electric field, I_{CARS} is the intensity of the anti-Stokes signal in the degenerate CARS, I_p is the intensity of the pump laser beam, and C is the constant that depends on the experimental conditions, which include the parameters of the medium and experimental setup. Finding the value of C is possible by performing the experiment in the given optical setup with a uniform and known electric field.

In Ref. [26] a polarization CARS technique for measuring the direction of the electric field was employed. In the case where the pump (ω_p) and Stokes (ω_s) laser beams have polarization in the same direction and create a certain angle with respect to the direction of the external electric field, one can reconstruct the angle between the electric field and the lasers' polarization directions, measuring the polarization of the generated IR signal [see Fig. 1(b)]. A convenient method of measuring the direction of an electric field by means of polarization CARS is to orient the axis of a polarization analyzer first parallel and then perpendicular to the polarizations of the lasers, which yields the intensities of the following components of the IR CARS signal:

$$\sqrt{I_{||}^{IR}} = C_1 E_\tau E_p E_s, \quad (2)$$

$$\sqrt{I_{\perp}^{IR}} = C_2 E_\eta E_p E_s, \quad (3)$$

where E_τ and E_η are the absolute values of the tangential and the normal components of the electric field vector (with

respect to the orientation of the lasers), respectively, E_p and E_s are the amplitudes of the pump and Stokes laser waves, respectively, and C_1 and C_2 are the constants, which can be determined, using a setup with an electric field of known strength and orientation. Once the amplitudes E_τ and E_η are calculated from the measurement, the electric field vector can be reconstructed via $\vec{E} = E_\tau \hat{\tau} + E_\eta \hat{\eta}$.

In our experiments, an all-solid-state generator [6] was employed, delivering HV pulses with a duration of ~ 5 ns at full width at half maximum (FWHM) and an amplitude of ~ 100 kV to the diode. The diode was preliminary evacuated (0.1 Pa) and then filled with H_2 gas at $P = 3 \times 10^5$ Pa or $P = 2 \times 10^5$ Pa. The discharge voltage and current waveforms were measured using a capacitive voltage divider and B dot, respectively. The cathode was made of a stainless steel blade with a length of 7 mm, and a width of several μm at its emitting edge. The anode, made of an Al disk of 150 mm in diameter, was located at distances $d_{CA} = 10$ mm and $d_{CA} = 20$ mm from the cathode. For the calibration experiment [27,28] with a known uniform electric field, instead of the blade cathode, a 40-mm diameter stainless steel disc connected to a dc power supply was used.

The laser beam ($\lambda = 532$ nm), generated by a Continuum Surelite III laser, was split to excite the dye (LD 688 dissolved in dimethyl sulfoxide) in a Continuum ND6000 laser and to supply the pump (ω_p) laser beam for CARS. The Stokes beam (ω_s) at $\lambda = 683$ nm, generated by the dye laser, was coaligned with the pump laser (see Fig. 2). Part of the pump laser beam was recorded with a photodiode (Thorlabs SM05PD2A), to monitor the beam intensity. The polarization of both the pump and Stokes beam was rotated using a multiorder half-wave plate to coincide with the direction of the cathode-anode axis. Both laser beams were focused at the interrogation spot in the discharge chamber using a lens. The duration of the laser beams was 4 ns at FWHM and the powers, measured at the input of the discharge chamber, were 40 and 3.5 mJ for the pump and Stokes beams, respectively. Anti-Stokes ($\lambda = 436$ nm) and IR ($\lambda = 2.4 \mu\text{m}$) radiation, formed at the location of the focus, emerged from the discharge chamber collinearly with the pump and Stokes beams. IR radiation was focused using a lens at the input window of the IR detector (Hamamatsu P5968-060). At the exit window of the chamber a blue filter was used to cut off the pump and dye laser beams. Behind the IR focusing lens a Ge filter was placed at an angle of 45° to deflect the anti-Stokes beam, which further was focused on a photodiode (Thorlabs SM05PD2A) to monitor the intensity of the CARS signal. To suppress the visible wavelengths and higher orders of the CARS signal, leaving only the IR radiation at $\lambda = 2.4 \mu\text{m}$, an additional pack of filters was placed in the front of the IR detector. In experiments where the orientation of the electric field was determined, a Glan-Thompson prism was employed as a polarization analyzer in front of the IR detector. The signals from the

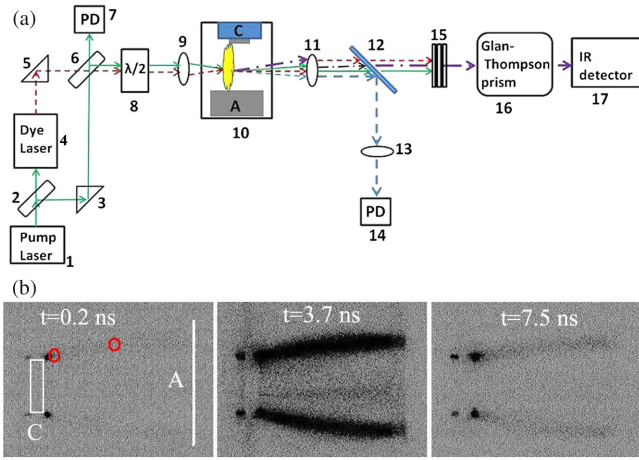


FIG. 2 (color online). (a) CARS setup. 1, pump laser; 2 and 6, beam splitters; 3 and 5, right angle prisms; 4, dye laser; 7 and 14, photodiodes; 8, multiorder half waveplate; 9, 11, and 13, lenses; 10, discharge chamber; 12, Ge filter; 15, filter stack; 16, Glan-Thompson prism; 17, IR detector. (b) Different evolution stages of the discharge channels in the He; shots taken with 4Quik fast framing camera; exposure time is 2 ns. Pressure $P = 3 \times 10^5$, $d_{CA} = 20$ mm. Red circles on the first frame indicate the two locations from which the signals in the experiments were collected ($d_C = 1$ mm and $d_C = 10$ mm).

photodiodes, IR detector, voltage divider, and B dot were recorded using a Tektronix digitizing oscilloscope (TDS 694C: 3 GHz, 10 gigasamples/s).

Time-resolved imaging of the light emission from the cathode-anode gap, obtained with a 4QuikE intensified fast framing camera, showed that discharges are initiated from the top and bottom edges of the cathode, apparently due to the enhancement of the electric field at those locations [see Fig. 2(b)]. Thus, to study the electric field evolution in the plasma channel, IR signals were collected from two locations: at the distance of 1 mm ($d_C = 1$ mm) from the cathode's top edge and from the middle of the discharge channel, i.e., 10 mm ($d_C = 10$ mm) away from the top edge of the cathode.

On average, a hundred shots were recorded for each set of experimental conditions (cathode-anode gap, gas pressure, and distance from the cathode), spanning the time period of ~ 20 ns with respect to the beginning of the discharge current. The temporal resolution of the diagnostics was determined by the duration of the laser pulses. Since the intensity of the CARS radiation $I_{aS} \sim I_p^2 I_S$ and the intensity of the IR radiation $I_{iR} \sim I_p I_S$ [23], one can consider that the results are primarily dependent on the intensity at the peak of the laser pulse, the duration of which is ~ 2 ns and, respectively, 2 ns was considered as the effective time resolution. A $t = 0$ time was set, where the voltage pulse reaches 30% of its amplitude and all the shots were assigned times of the CARS signal onset with respect to $t = 0$. Subsequently, shots were divided into groups belonging to 1 ns duration time intervals, and the

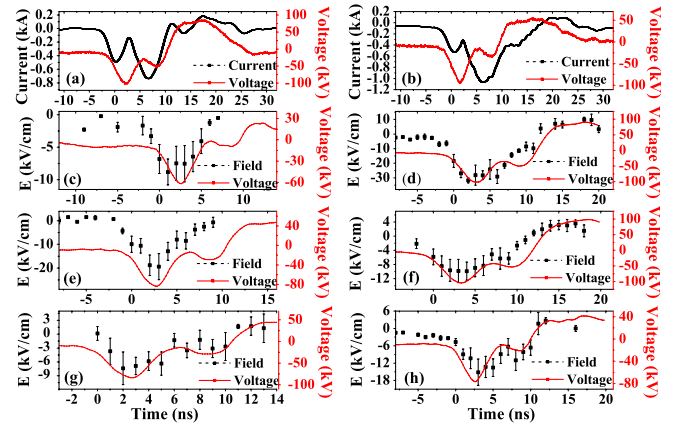


FIG. 3 (color online). Voltage and current waveforms: (a) $d_{CA} = 20$ mm, $P = 3 \times 10^5$ Pa, (b) $d_{CA} = 20$ mm, $P = 2 \times 10^5$ Pa. Measured electric field and the voltage pulse under different conditions: (c) $d_{CA} = 10$ mm, $P = 3 \times 10^5$ Pa, $d_C = 1$ mm, (d) $d_{CA} = 20$ mm, $P = 3 \times 10^5$ Pa, $d_C = 1$ mm, (e) $d_{CA} = 20$ mm, $P = 2 \times 10^5$ Pa, $d_C = 1$ mm, (f) $d_{CA} = 20$ mm, $P = 3 \times 10^5$ Pa, $d_C = 10$ mm, (g) $d_{CA} = 10$ mm, $P = 2 \times 10^5$ Pa, $d_C = 1$ mm, (h) $d_{CA} = 20$ mm, $P = 2 \times 10^5$ Pa, $d_C = 10$ mm.

amplitudes in each time interval were averaged to represent an averaged signal for this time interval.

The temporal evolution of the electric field at the distances of 1 ± 0.5 and 10 ± 0.5 mm from the cathode for different pressures and cathode-anode gaps with the corresponding measured voltage and integrated B-dot current waveforms is shown in Fig. 3. The presented voltage and current waveforms for $d_{CA} = 20$ mm differ insignificantly from those obtained for $d_{CA} = 10$ mm; namely, in the latter case the amplitude of the voltage was $\sim 20\%$ smaller and that of the current $\sim 30\%$ larger. Also, the presented voltage waveform was not corrected for inductive voltage $LdI/dt \leq 20$ kV, where L is the inductance of the cathode holder.

The most obvious observation is the presence of a significant electric field in the plasma channel with peak values up to $E = 30$ kV/cm. The electric field evolution follows closely the waveform of the HV pulse applied to the cathode-anode gap, with both approaching their peaks simultaneously. Another result is that the electric field in the vicinity of the cathode is comparable to or even lower than the one measured in the middle of the discharge channel. One can suppose that the enhancement of the electric field due to the geometry is compensated by the greater density of the plasma at that location, resulting in a lower electric field penetrating the plasma. In addition, a very important observation is that the rms values of the electric field are similar to ones calculated via the fitting of He I spectral lines [15]. The presence of such high electric fields inside the discharge channel shows that the plasma produced in nanosecond discharges is highly resistive, and it cannot acquire the cathode potential to the head of the

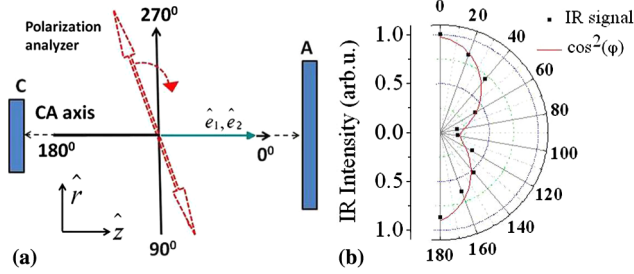


FIG. 4 (color online). (a) Orientation of the laser waves relatively to the cathode-anode axis and the schematic rotation of the polarization analyzer, (b) IR signal dependence on the angle of the polarization analyzer (φ): experimental results and a $\cos^2(\varphi)$ fit.

propagating plasma channel. One can also estimate the density of the plasma based on the measured electric field and assuming low-ionized plasma where electron-neutral collisions play a dominant role [29]:

$$n_e \approx 3.6 \times 10^{16} I n_n V_e \sigma_{tr} (SE)^{-1} \approx 10^{15} - 10^{16} \text{ cm}^{-3}, \quad (4)$$

where $I \approx 800$ A is the discharge current, $S \approx 0.08$ cm² is the cross-sectional area of two discharge channels which was estimated using side- and front-view time-resolved images of the discharge channel, $E \leq 30$ kV/cm is the electric field, $n_n \approx 6 \times 10^{19}$ cm⁻³ is the neutral density, $V_e \approx 10^8$ cm/s is the average thermal velocity of electrons for temperature $T_e \leq 2$ eV [15], and $\sigma_{tr} \approx 10^{-15} - 10^{-16}$ cm² [29] is the collision electron-neutral transport cross section. This rather rough estimate is also in satisfactorily good agreement with the values of the plasma electron density obtained using time- and space-resolved spectroscopy studies [15]. The large resistivity of the plasma can be explained by the high frequency ($\nu_m \approx 2 \times 10^{12}$ s⁻¹) of the electron-neutral collisions, which are several orders larger in frequency than the frequency of the electron-ion ion collisions. Thus, one can estimate the resistivity of this low-ionized plasma as [29] $\sigma = 2.82 \times 10^{-4} n_e [\text{cm}^{-3}] \nu_m^{-1} [\text{s}^{-1}] \approx 0.5 \Omega^{-1} \text{ cm}^{-1}$ and the average resistance of the discharge channels as $R_{ch} = \sigma^{-1} l S^{-2} \approx 75 \Omega$ for an effective length of the plasma channel $l \approx 3$ cm. This rough estimate also agrees satisfactory with the average resistance of the discharge channel at $t \approx 2.5$ ns calculated as $R = V/I \leq 70 \Omega$ where V and I are the diode voltage and current, respectively.

In order to find the direction of the external electric field, the dependence of the IR intensity on the angle of the polarization analyzer placed at the entrance of the IR detector was obtained. The Glan-Thompson prism was rotated in intervals of 10°, throughout 180° [see Fig. 4(a)]. At each angle intervals 50 shots with maximal IR amplitudes and shot times falling in the same time interval of ~ 2 ns duration were recorded. These signals were averaged to represent the signal level for the given angle [see Fig. 4(b)]. One can see that the IR intensity nearly vanishes at $\sim 90^\circ$, when the orientation of

the polarization analyzer is perpendicular to that of the laser waves, hence, implying $E_\eta \ll E_r$, i.e., that the electric field orientation is nearly collinear with that of the lasers.

To summarize, the results obtained using the CARS method show the existence of an electric field with rms values of up to tens of kilovolts per centimeter, directed mainly along the cathode-anode axis in the plasma channel during a nanosecond time scale discharge in H_2 gas at $P = (2-3) \times 10^5$ Pa. The found electric field with an amplitude of several tens of kilovolts agrees with the results reported in Ref. [15] and shows that the plasma channel presents low-ionized plasma characterized by a rather larger resistivity. The high value of the electric field obtained can be explained by the high frequency of the electron-neutral collisions. However, this electric field is not sufficient for the formation of RAE in H_2 gas from electrons produced in bulk in the plasma channel because there is not sufficient energy and the length of the cathode-anode gap is only a few centimeters [30]. The obtained evolution of the electric field in the discharge channel of a nanosecond time scale discharge is of great importance because it makes doubtful the suggestion [3,4,12] of the possible emission of RAE from the head of the plasma boundary propagating toward the anode, in this gas. Also, the high resistivity of the nanosecond-time scale discharge in a pressurized gas leads to a large energy dissipation, which should be accounted for in different devices where such a type of discharge is used.

-
- [1] P. Babich and T. V. Loiko, *Plasma Phys. Rep.* **36**, 263 (2010).
 - [2] G. A. Mesyats, M. I. Yalandin, A. G. Reutova, K. A. Sharypovb, V. G. Shpakb, and S. A. Shunailov, *Plasma Phys. Rep.* **38**, 29, (2012).
 - [3] V. F. Tarasenko, *Plasma Phys. Rep.* **37**, 409 (2011).
 - [4] V. F. Tarasenko and S. I. Yakovlenko, *Plasma Devices Oper.* **13**, 231 (2005).
 - [5] S. Yatom, J. Z. Gleizer, D. Levko, V. Vekselman, V. Gurovich, E. Hupf, Y. Hadas, and Ya. E. Krasik, *Europhys. Lett.* **96**, 65 001 (2011).
 - [6] S. Yatom, V. Vekselman, J. Z. Gleizer, and Y. E. Krasik, *J. Appl. Phys.* **109**, 073312 (2011).
 - [7] S. Yatom, V. Vekselman, and Ya. E. Krasik, *Phys. Plasmas* **19**, 123507 (2012).
 - [8] A. V. Gurevich, G. A. Mesyats, K. P. Zybin, M. I. Yalandin, A. G. Reutova, V. G. Shpak, and S. A. Shunailov, *Phys. Rev. Lett.* **109**, 085002 (2012).
 - [9] L. P. Babich, T. V. Loiko, and V. A. Tsukerman, *Sov. Phys. Usp.* **33**, 521 (1990).
 - [10] G. A. Mesyats, *JETP Lett.* **85**, 109 (2007).
 - [11] G. A. Mesyats and M. I. Yalandin, *IEEE Trans. Plasma Sci.* **37**, 785 (2009).
 - [12] S. Yatom, D. Levko, J. Z. Gleizer, V. Vekselman, and Ya. E. Krasik, *Appl. Phys. Lett.* **100**, 024101 (2012).
 - [13] A. N. Tkachev and S. I. Yakovlenko, *Central Eur. J. Phys.* **2**, 579 (2004).

- [14] D. A. Sorokin, M. I. Lomaev, and K. Yu. Krivonogova, News Tomsk Polytechnic University **316**, 18 (2010) (in Russian).
- [15] S. Yatom, E. Stambulchik, V. Vekselman, and Ya. E. Krasik, Phys. Rev. E **88**, 013107 (2013).
- [16] C. A. Moore, G. P. Davis, and R. A. Gottscho, Phys. Rev. Lett. **52**, 538 (1984).
- [17] B. N. Ganguly and A. Garscadden, Phys. Rev. A **32**, 2544 (1985).
- [18] U. Czarnetzki, D. Luggenholscher, and H. F. Döbele, Phys. Rev. Lett. **81**, 4592 (1998).
- [19] E. U. Condon, Phys. Rev. **41**, 759 (1932).
- [20] M. F. Crawford, H. L. Welsh, and J. L. Locke, Phys. Rev. **75**, 1607 (1949).
- [21] A. N. Dharamsi and K. H. Schoenbach, J. Appl. Phys. **69**, 2889 (1991).
- [22] V. P. Gavrilenko, E. B. Kupriyanova, D. P. Okolokulak, V. N. Ochkin, S. Yu. Savinov, S. N. Tskhai, and A. N. Yarashev, Pis'ma. Zh. Eksp. Teor. Fiz. **56**, 3 (1992).
- [23] O. A. Evsin, E. B. Kupryanova, V. N. Ochkin, S. Yu. Savinov, and S. N. Tskhai, Quantum Electron. **25**, 278 (1995).
- [24] T. Ito, T. Kanazawa, and S. Hamaguchi, Phys. Rev. Lett. **107**, 065002 (2011).
- [25] V. N. Ochkin and S. N. Tskhai, Phys. Usp. **46**, 1214 (2003).
- [26] S. N. Tskhai, D. A. Akimov, S. V. Mitko, V. N. Ochkin, A. Yu. Serdyuchenko, D. A. Sidorov-Biryukov, D. V. Sinyaev, and A. M. Zheltikov, J. Raman Spectrosc. **32**, 177 (2001).
- [27] T. Ito, K. Kobayashi, U. Czarnetzki, and S. Hamaguchi, J. Phys. D **43**, 062001 (2010).
- [28] D. A. Akimov, A. M. Zheltikov, N. I. Koroteev, A. N. Naumov, A. Yu. Serdyuchenko, D. A. Sidorov-Biryukov, and A. B. Fedotov, JETP Lett. **70**, 375 (1999).
- [29] Yu. P. Raizer, *Gas Discharge Physics* (Springer-Verlag Berlin, Berlin, 1997).
- [30] A. V. Gurevich and K. P. Zybin, Phys. Usp. **11**, 1110 (2001).